

## CHAPTER-4

### NUMERICAL ANALYSIS AND DISCUSSION

Numerical analysis is an important tool for understanding the behavior of structures. STAADPro v8i is the most widely used tool for the design and analysis of civil engineering structures hence, the numerical study was done on STAAD.Pro v8i. The observations recorded from the experiments of composite and non-composite models were used to validate the numerical models of the structure.

#### 4.1 NUMERICAL ANALYSIS OF MODELS

The bridge models tested in the laboratory were modelled on STAAD.Pro v8i software. Analysis was performed on non-composite and composite models and their STAAD editor files are attached as annexure A and B. The objective of the analysis was to find the correlation between numerical results from STAAD and results obtained from experimental data.

##### 4.1.1 Non-composite models

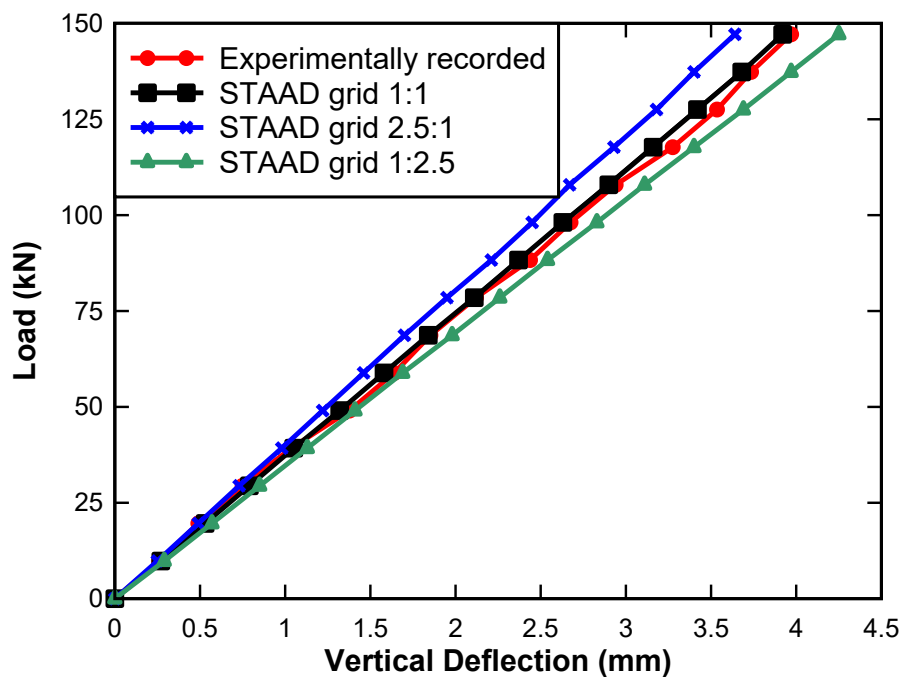
For modelling the non-composite model the members of the frame were taken as beam elements in STAAD.Pro. The material properties were taken from the material tests performed in the laboratory. The experimentally observed values of vertical deflection and strain in the compressive top cord members of the truss model were compared with the STAAD models and curves showed good correspondence. The average vertical deflection from the dial gauges at a load of 44 kN was 1.99mm which is close to deflection observed numerically, which is 2.09mm. This close resemblance between numerical and experimental results validates the STAAD model.

### 4.1.2 Composite model

The composite bridge was modelled on STAAD.Pro V8i software. All the steel members were modelled as beam elements, and four noded plate elements were used for modelling the RCC deck slab. The meshing of the deck slab was done in different sizes and ratios. At first, the ratio of the grid sizes was tested against the experimentally recorded data. The grid ratios taken for the analysis are as follows

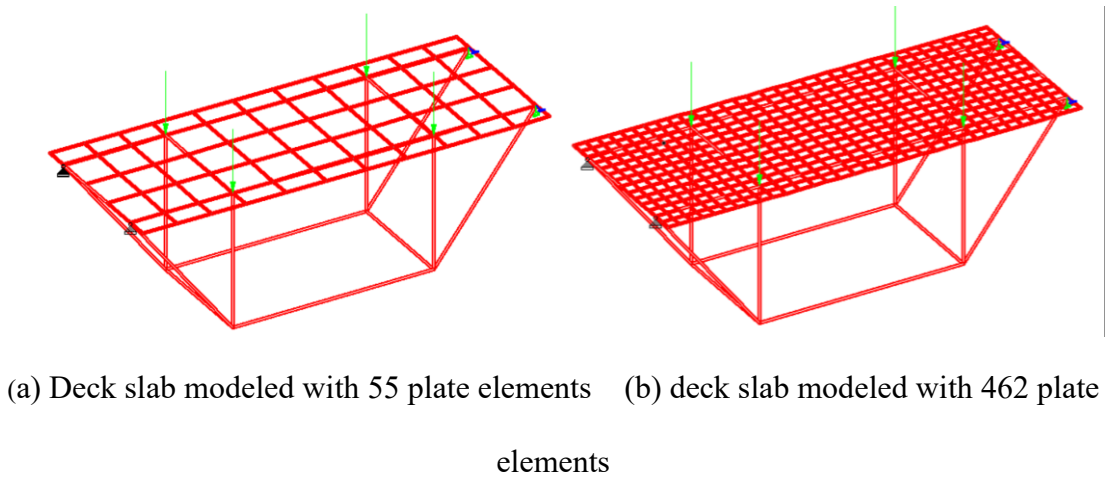
1. L: B ratio as 1:1
2. L: B ratio as 2.5:1
3. L: B ratio as 1:2.5

Figure 4.1 shows the variation of vertical deflection of the model as obtained from the STAAD models with different mesh shapes and experimental deflection. From the Figure, it is seen that the mesh shape with L: B variation of 1:1 yields the closest result to the experimentally observed deflections.



**Figure 4.1** Variation of vertical deflection as obtained from various grid sizes of STAAD and experimental deflection

The concrete deck was then modelled in 1:1 four noded plate elements. The size of the mesh was then altered to observe the effect of change in size on the deflection. The deck was then divided into two different mesh sizes as shown in Figure 4.2. Figure 4.2.a shows the deck slab with 55 plate elements and 4.2.b shows the deck slab divided into 462 meshes. The resulting deflections are compared and are shown in Figure 4.3.



**Figure 4.2** Meshing of the deck slab

The deflection of the composite models with the above two meshes of the deck slab is compared in Figure 4.3

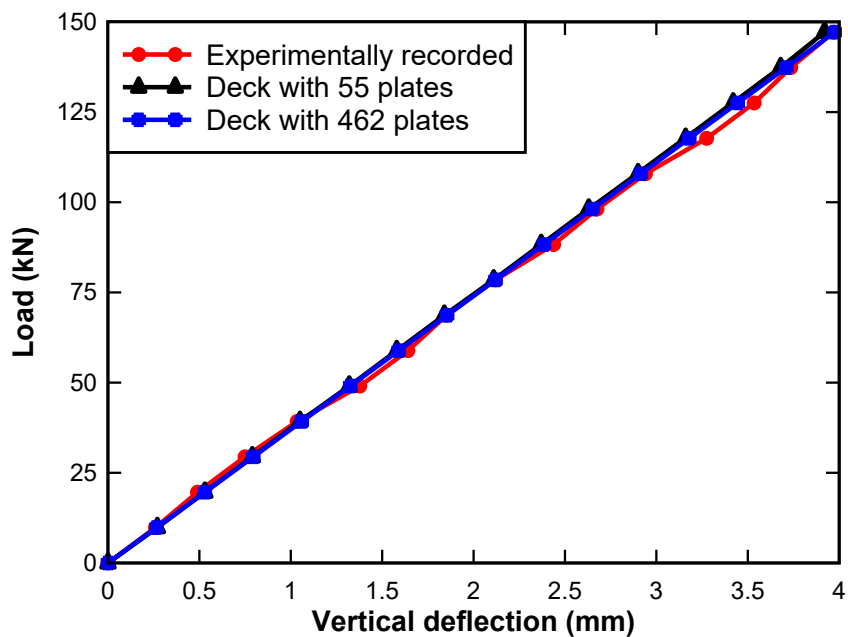


**Figure 4.3** Vertical deflections of the truss

From the figure, it is clear that the mesh size of the deck slab has little effect on the analysis results provided the aspect ratio of the elements be near one. For further discussions, a deck slab with 461 elements is used.

The concrete used in the STAAD model is modeled using linear elastic model. The parameters used in the modeling of deck slab are as follows:

$F_{cu} = 50 \text{ N/mm}^2$ ;  $E = 35355.34 \text{ N/mm}^2$ ; Poisson's Ratio = 0.17; Density =  $2500 \text{ kg/m}^3$

#### **4.2 EFFECT OF SHRINKAGE STRAIN**

In the deck type composite steel open web girder bridge, steel structure is first launched, and then casting of deck slab takes place and after that, superimposed dead loads (SIDL) are applied. After casting and hardening the deck slab, the bridge is open to traffic. During hardening of concrete in deck slab, shrinkage cracks initiate. Shrinkage has following effects on RCC decks.

1. Shrinkage of concrete between movement joints causes joints to open or make it wider.
2. Where other materials such as ceramic tiles are fixed on top of concrete surface, shrinkage of concrete causes relative motion between different materials. The resulting stresses can cause failure at the interface.
3. If shrinkage is restrained, the concrete is put into tension and when tensile stresses become equal to the tensile strength, the concrete cracks.
4. The deflection of flexural members is increased by shrinkage. This is because the lightly reinforced compression zone is free to shrink more than heavily reinforced tension zone.
5. Shrinkage causes reduction in pre-stressing force.

6. Shrinkage of concrete causes the concrete to grip reinforcing bars (especially plain bars) more tightly. This increases friction between concrete and steel hence improving bond strength.

Shrinkage strain of the deck slab concrete may not permit composite action of RCC deck with the top chord members of the steel open web girder bridge until it is overcome by the flexural strain under the live load or overload condition. Reinforcement present in the RCC deck resists the initiation of shrinkage cracks to some extent. However, it is important to examine the extent of composite action between RCC deck and steel open web girder bridge until strain in the deck slab under live load or overload condition exceeds the shrinkage strain. Shrinkage strain in M40 grade deck slab concrete may be taken as 0.0003 (Clause discussed below). Cl. No 6.2.4.1 (IS 456-2000) In the absence of test data, the approximate value of the total shrinkage strain for design may be taken as 0.0003 (for more information, refer-IS 1343).

Cl. No. 5.2.4.1 (IS 1343-1980) In the absence of test data, the approximate value of shrinkage strain for design shall be assumed as follows:

For pre-tensioning = 0.0003

$$\text{For post-tensioning} = \frac{0.0002}{\text{Log}_{10}(t+2)} \quad (4.1)$$

Where t = age of concrete at transfer in days.

NOTE — The value of shrinkage strain for design of post-tensioned concrete may be increased by 50 percent in dry atmospheric conditions, subject to a maximum value of 0.0003.

Due to shrinkage, micro-cracks develop in concrete and hence concrete starts taking load only after these micro-cracks are closed due to induced flexural stresses. Therefore, it is assumed that composite action between the RCC deck and steel open web girder may not take place until strain in the deck slab concrete exceeds 0.0003.

Strain variation under different loads with shrinkage effect for a composite open web girder bridge is shown in Figure 4.4. After hardening of deck slab, due to shrinkage strain ( $\epsilon_{sh}$ ) total dead load is carried by steel open web girder only. During live load, there is a further increase in strain in the top chord as well bottom chord members. In this stage, some part of shrinkage strain in the deck slab is overcome due to flexural strain. As the live load on the bridge goes on increasing in an overload condition, the remaining shrinkage strain ( $\epsilon_{sh} - \epsilon_{LL1}$ ) shall overcome by flexural strain in deck slab and composite action between RCC deck and steel open web girder starts taking place. During overload condition or at plastic condition, neutral axis shifts in deck slab and compression shall be carried by RCC deck only.

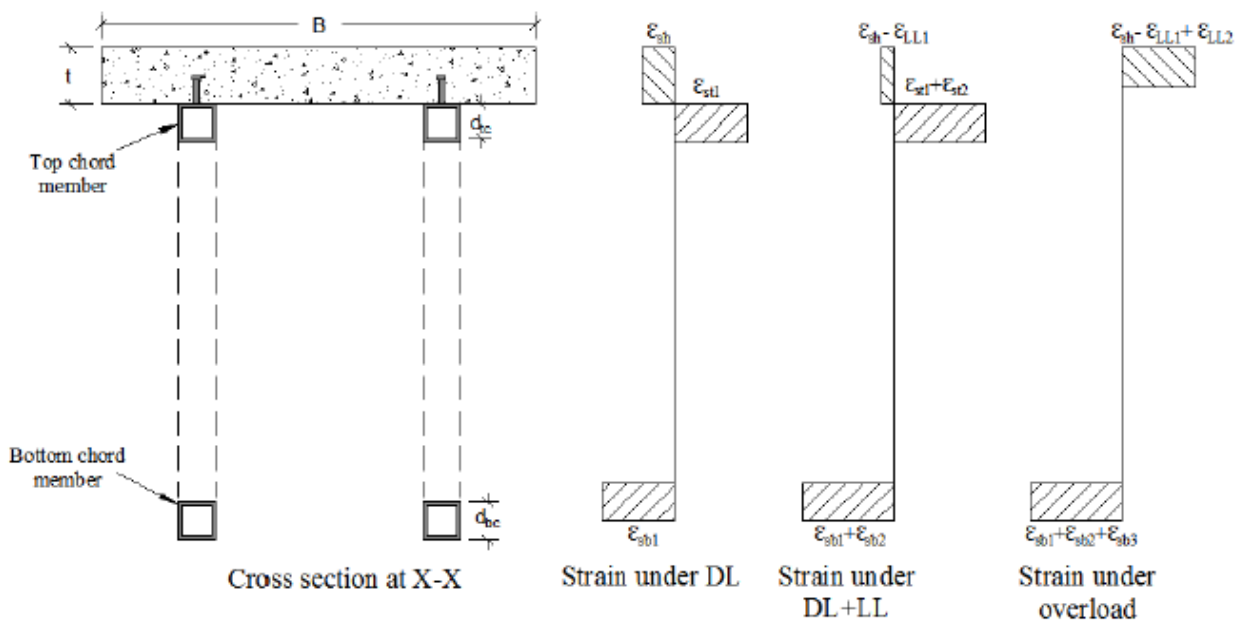


**Figure 4.4** Strain diagram

Following is the STAAD.Pro analysis of deck slabs of 2 different bridges under live load condition.

1. A 30m span steel open web girder bridge (Two lane) across stream on left bank of river Bhagirathi for IRC Class-A and 70-R loading at Kotibhel, Uttrakhand (Figure 4.5).

Span length = 30.0 m

Span width = 7.9 m

Height of bridge = 7.5 m

The following is the elevation of the bridge

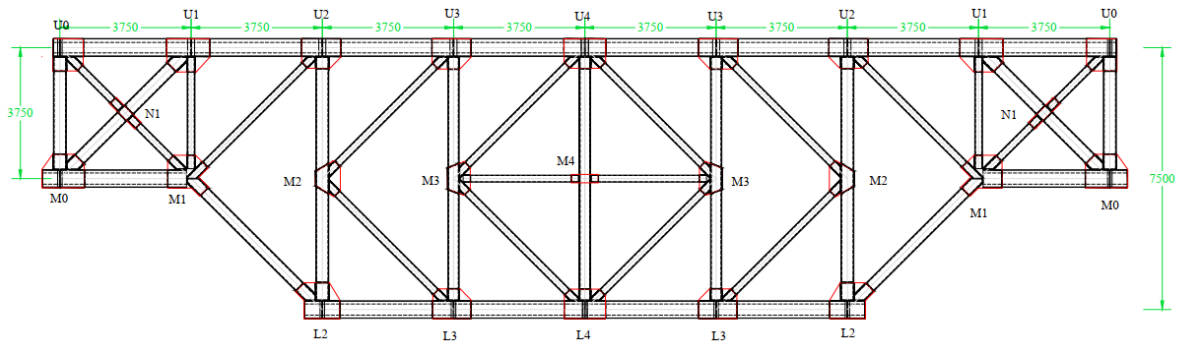


**Figure 4.5:** Elevation of 30 m span bridge used for analysis.

The bridge was analyzed in STAAD.Pro under live load condition for getting stress contours in deck slab as shown in Figure 4.6.

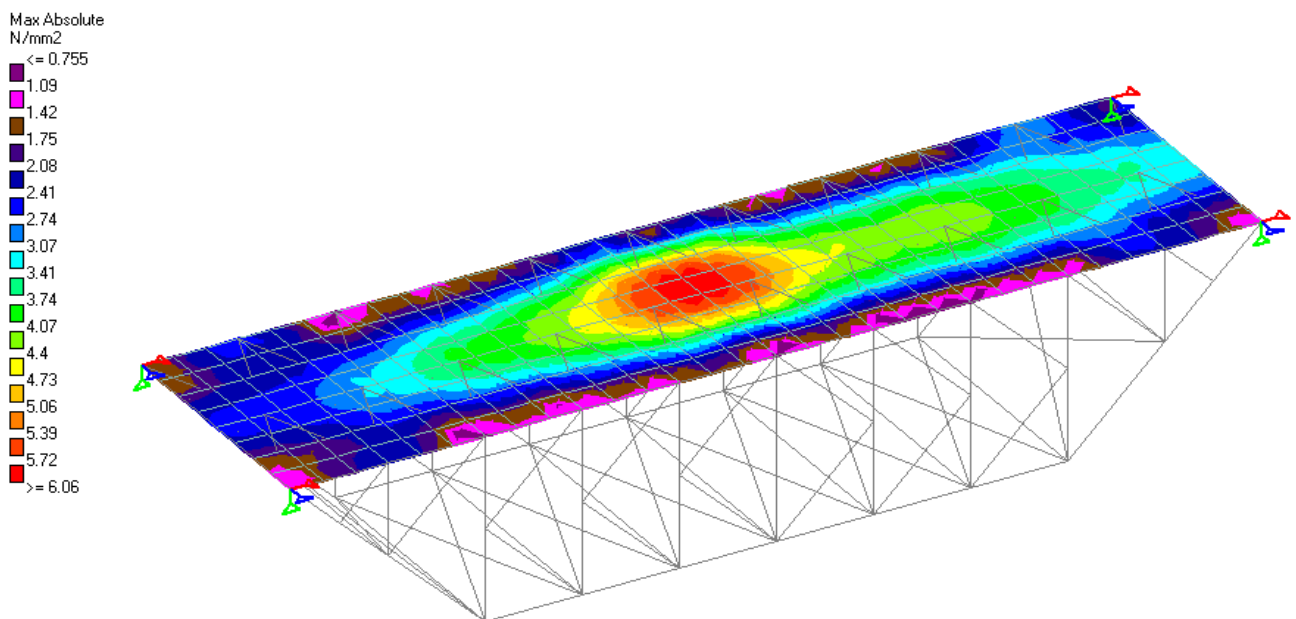


**Figure 4.6:** Stress contour of 30 m span bridge analyzed for live load condition in STAAD.Pro

In analysis, the maximum stress of  $6.06 \text{ N/mm}^2$  was observed at the middle span of the bridge, which leads to a strain of 0.00019, which is less than 0.0003 (indicated by the code). Therefore, composite action in the bridge may not take place even under full-service load conditions.

2. A 42m span steel open web girder bridge on Devidhar-Fold to Bhatwadi-Panchangaon Road at Uttarkashi, Uttrakhand

Geometric details of a 42m span bridge are given below.

Height of open web girder (C/C distance between top chord and bottom chord members) = 7m

C/C distance between two trusses = 4.85 m

Width of roadway = 4.25 m

Panel length = 3.5m

Number of 3.5m top panels = 12

Number of 3.5m bottom panels = 8

C/C distance between cross girders = 3.5m

Elevation of the analyzed bridge model is given in Figure. 4.7.

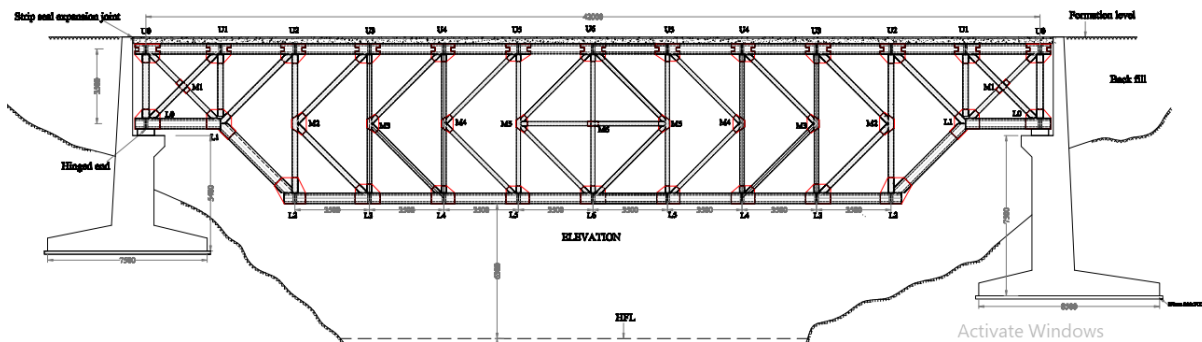


Figure 4.7: Elevation of 42m span bridge

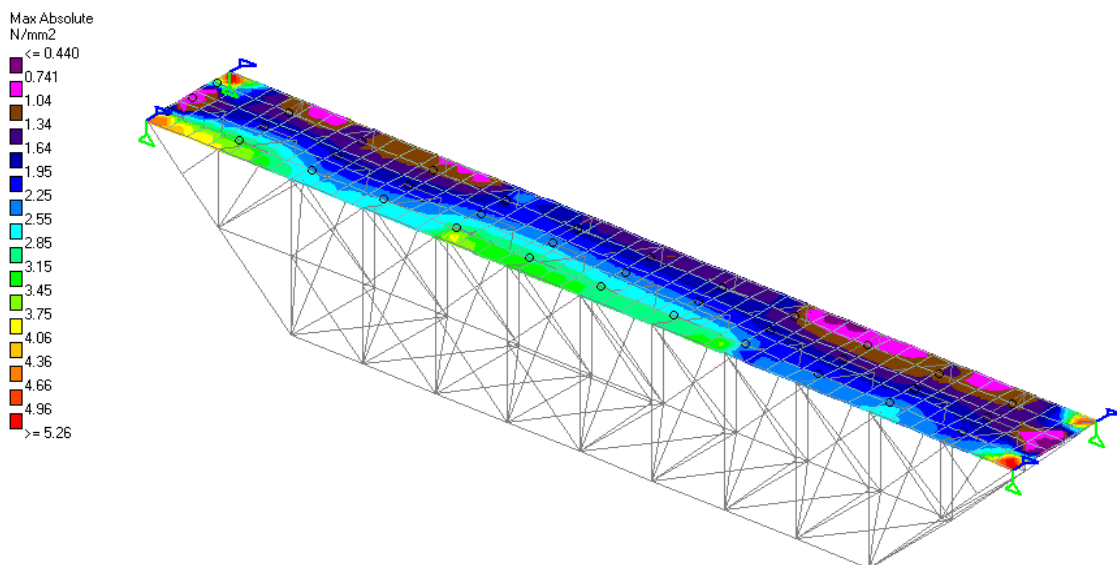
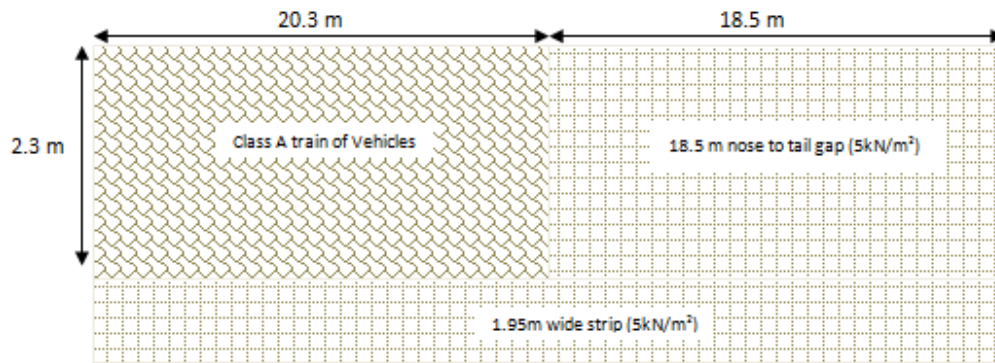


Figure 4.8: Deck slab stress under II alone

The deck slab is modeled using plate elements, which are connected over the two trusses at every 0.5m interval with the help of rigid studs in four rows (Figure 4.8). STAAD.Pro V8i software has been used for modeling and analysis. As per the STAAD analysis result, the maximum stress in the deck slab concrete at mid-span for live load with impact alone is found to be  $4.06 \text{ N/mm}^2$  (Figure 4.9).

The strain corresponding to  $4.06 \text{ N/mm}^2$  stress is 0.00013, which is far below the 0.0003 deck slab shrinkage strain. Therefore, composite action in structure may not be possible even under full-service load conditions.



**Figure 4.9:** Loading arrangement for fully loaded deck slab.

Although, composite action between a deck slab and an open web girder may not be possible in the service condition. Nevertheless, due to the presence of reinforcement in the deck slab, some participation may be there from the beginning. Due to shear connectors, top chord compression members of the open web steel girder will be laterally supported by the connected RCC deck and their lateral buckling may be prevented. Thereby, higher compressive stress than the buckling stress, up to the ultimate compressive strength, may take place in these members, provided web members are designed to remain safe.

### 4.3 DISCUSSION

The results obtained from laboratory tests and numerical analysis have indicated the following notable points.

#### 4.3.1 Validation of the STAAD results.

The FEM analysis procedure is widely applicable for the analysis of different types of structures, and therefore it was used here to analyze the composite model. To validate the numerical findings using the FEM analysis the following checks are applied.

- i. The bottom chord strain is calibrated using the electrical strain gauge results.  
(Figure 4.10)
- ii. The steel top chord strain is validated using the electrical strain gauge results.  
(Figure 4.11)
- iii. The deflection at the mid-span is calibrated using the experimental results.  
(Figure 4.12)
- iv. The strain recorded in the deck slab is also compared with numerical results  
(Figure 4.13)

#### *Strain in the bottom chord*

The analyzed strains by using the STAAD model and the experimentally recorded strain in the bottom chord and are compared in Figure 4.10.

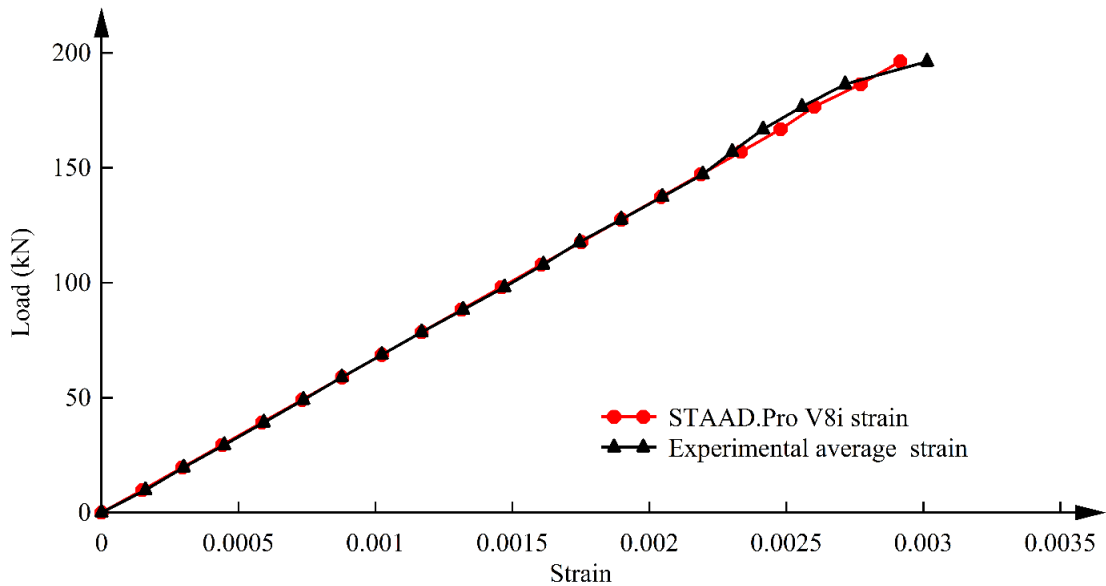


**Figure 4.10** Strain in the bottom chord

Comparison of the strains obtained from the STAAD analysis and the average experimentally recorded strain and at various loading stages are seen to closely tally. Thus, the STAAD model results for the bottom chord strain are calibrated.

*Strain in the top chord*

Total compression in the composite top chord at the mid-span of the truss must be equal to the tension in the bottom chord. Total compression in the composite top chord comprises compression in the deck concrete, reinforcing steel in the deck, and the steel top chord member. At any stage of loading, compressive forces in the three components of the top chord are suitably adjusted to keep the total compressive force equal to the tensile force in the bottom chord.

Strain variation in the steel top chord members, as found from the STAAD analysis and average strain obtained from the experiment, is shown in Figure 4.11.

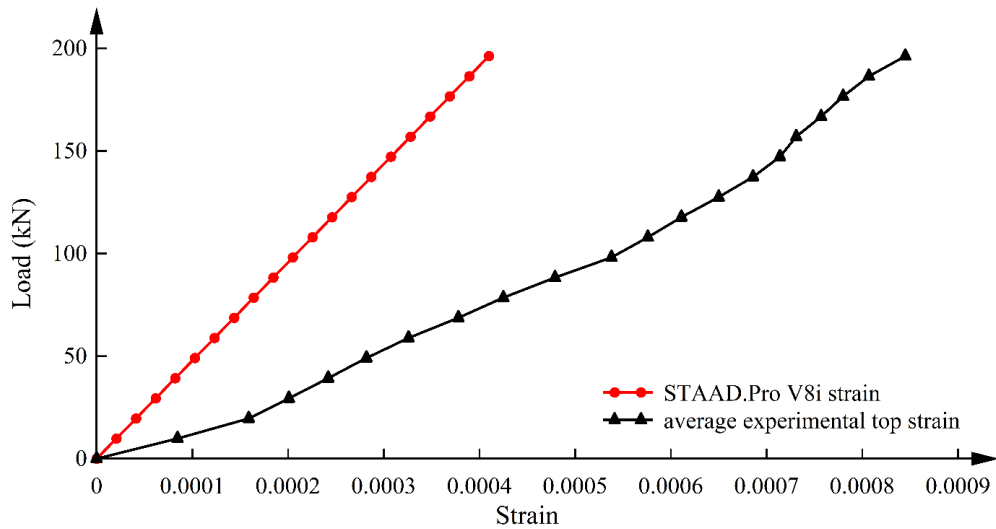


**Figure 4.11** Strain in the steel top chord

The experimentally recorded strain is higher by about 100% than the STAAD analysis strains. This is due to the presence of shrinkage cracks in the concrete deck slab.

*Deflection at mid-span*

Experimental and numerical deflections of the composite model at the mid-span of the model are shown in Figure 4.12.

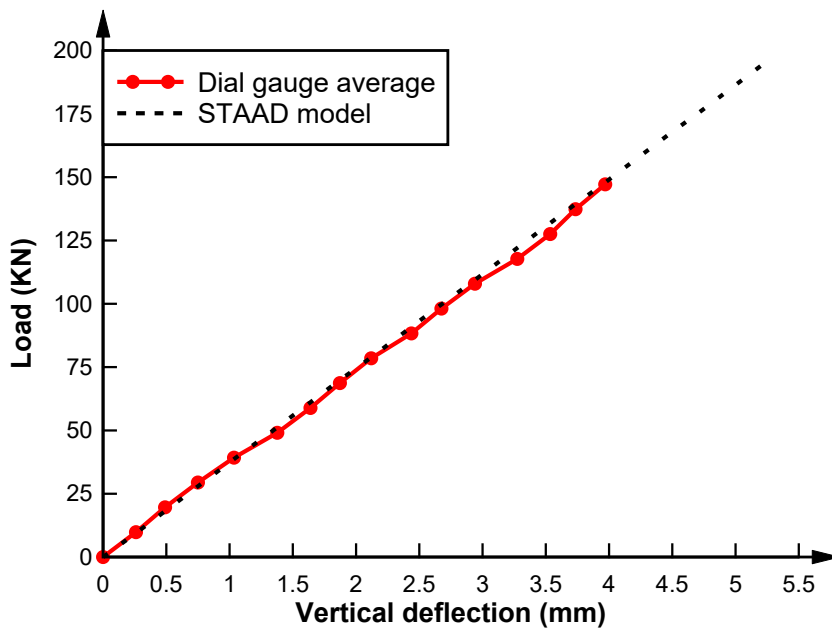


**Figure 4.12** Deflection of the bridge model.

The bridge model failed at 196.2 kN. Vertical deflection recorded at 147kN is 3.97 mm. Experimental deflection in Figure 4.12 is seen to closely tally with the linear STAAD model result. Therefore, deflection found from the STAAD model analysis is calibrated.

#### *Strain in the deck slab*

The strain in the deck slab was recorded using five strain gauges mounted at 6.5 cm centre to centre from each other (Figure 3.23). The plot of the strains recorded at various loading stages is shown in Figure 4.13 in solid lines. Strains obtained for the STAAD analysis are shown in dotted lines in Figure 4.13. The average strain in the deck slab at the failure load of 196.2 kN is 0.000431 which is 0.72 times the maximum strain. This indicates that the deck slab at failure fully participates in the composite action.

Strain in the deck slab significantly reduces from maximum strain at the truss locations from 0.00058 to minimum strain at the mid-section as 0.00026, which is reduced by 54.0%. Deck slab top view after failure is shown in Figure 3.26. From the figure, it is clear that there is no adverse cracking or crushing of the deck slab at any location. Strain at the centre of the deck as measured by strain gauge is 0.000265 and as per STAAD analysis, it is 0.000258. Therefore, the strains in the deck slab as found by experiment and analysis by STAAD tally with each other.

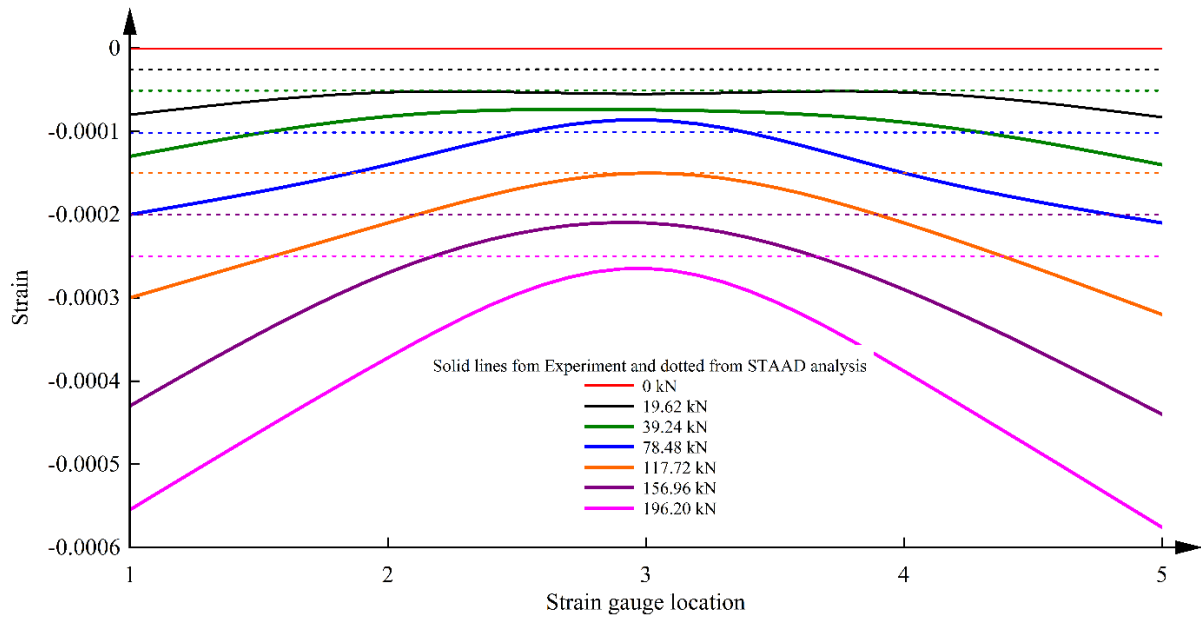


**Figure 4.13** Variation of deck slab strain

### 4.3.2 Load-deflection relationship

Load-deflection curves for the non-composite model and the composite model are shown in Figure 4.14. Deflections of both the bridge models are approximately linear. Shrinkage cracks are not considered in the deck modeled in STAAD. The linear deflection of the composite bridge model indicates that shrinkage cracks in the deck slab have little effect on its load-carrying capacity. At any load, total compression in the composite top chord is shared by the steel top chord member and the RCC deck slab. Thus, any deficiency in the load sharing by the cracked RCC deck due to its shrinkage is adequately overcome by the steel top chord member.

Comparing deflections at the common load of 44 kN, the ratio of deflections for the composite bridge model and non-composite model is 0.59. This shows better performance of the composite model by serviceability criteria.

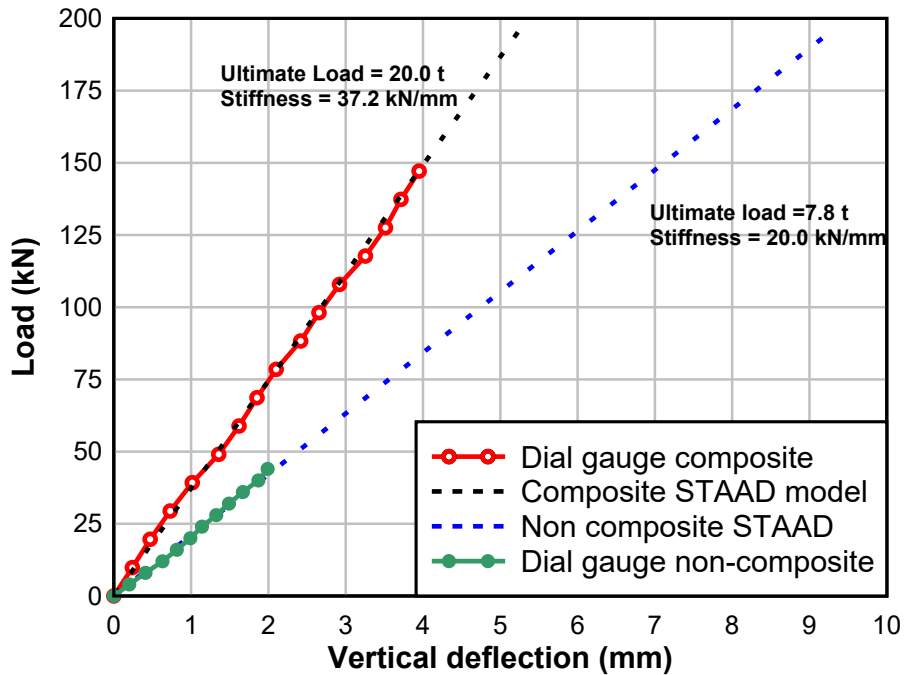


**Figure 4.14:** Load-Deflection relationship for composite and non-composite models.

### 4.3.3 Load carrying capacity

The ultimate load at failure for the truss bridge model is 76.5 kN and for the composite bridge model, it is 196.2 kN. Therefore, the load-carrying capacity for the composite bridge is 2.56 times that of the truss bridge. This increase in the load-carrying capacity is attributed to the role of the deck slab in preventing buckling of the deck slab. Due to this, the materials used in the model are used more efficiently.

### 4.3.4 Stiffness

The stiffness of the composite bridge is 37.2 kN/mm and for the truss, it is 20.0 kN/mm (Figure 4.14). Therefore, the stiffness of the composite bridge is 1.86 times the stiffness of the corresponding truss bridge, which may vary depending on the size of the deck slab the truss size. The significant change in stiffness against vertical loading will provide better serviceability of the bridge and reduce vibration of the bridge under live loading. Horizontal stiffness although not estimated through experiment, will surely improve due

diaphragm action by the composite slab. This will be effective against lateral loadings of wind and earthquake.

#### **4.3.5 Mode of failure**

Whereas the truss bridge model failed due to buckling of its top chord members at a load of 76.5 kN, the mode of failure for the composite bridge model entirely changed to rupture of the bottom chord members at a much higher load of 196.2kN.

Buckling failure of a bridge is highly undesirable as it is sudden. The composite bridge model gradually failed due to yielding and rupture of the bottom chord members at a much higher stress of 614.8 N/mm<sup>2</sup> in comparison to buckling failure of top chord members at a stress of 234.6 N/mm<sup>2</sup>. Thus, composite bridges may allow design with higher reserve strength and results in more economic design.

Due to load sharing by the RCC deck along with the load taken by the steel top-chord member, maximum stress in the top chord member is limited to 168.0 N/mm<sup>2</sup>, which is lower than the top chord buckling stress of 234.6 N/mm<sup>2</sup>. Therefore, the buckling of the top chord compression member was eliminated in the composite model.

#### **4.3.6 Load sharing between steel top chord and the RCC deck slab**

Both, the top chord as well as bottom chord members of the model consisted of 8mm x 8mm square steel bars. Therefore, in the symmetrical truss bridge model force carried by the top chord and bottom chord members is equal. Similarly, in the case of the composite bridge model also, the tensile force carried by the bottom chord member must be equal to the compressive force carried by the top chord and the RCC deck jointly.

The load was gradually increased at a constant rate during the test. Force in bottom chord members, top chord members and deck slab all increased with increment in load on the model. Member force distribution is calculated as :

At all equilibrium stages,

Net Compression force in top members = Net tensile force in lower members.

For top and bottom members, force in members is calculated from the strain recorded in the member. The difference between the both will be taken by the reinforcement and the deck concrete.

$$F_{\text{deck (reinforcement + concrete)}} = F_{\text{bottom}} - F_{\text{top}}$$

Assuming there is no slip between the reinforcement and deck concrete, the reinforcement will also experience the same average strain as experienced by the deck. Hence the force taken by reinforcement can be calculated accordingly. Force in the concrete of the deck slab is

$$F_{\text{concrete}} = F_{\text{deck}} - F_{\text{reinforcement}}$$

Member forces in the bottom chord and top chord were calculated from the respectively recorded strains (Figure 4.15). The deck slab compressive force is calculated as the difference between the top chord compressive force and bottom chord tensile force, which is shown in Figure 4.15. The deck slab, including concrete and the reinforcing steel, takes 72.0 % of the total compression in the composite top chord and the remaining 28.0% was taken by the top chord member.

Assuming that the reinforcement has the same strain as the surrounding concrete in the deck slab, force taken by the cracked deck slab concrete was calculated as the difference between the total force taken by the two and the force taken by the reinforcement alone. Therefore, at the failure, 30.7% of the total RCC deck force was taken by the reinforcing steel.

From the figure, it can also be noticed that, in the initial phase, the load taken by the reinforcement is greater than the load taken by the deck slab. This is perhaps due to the closing of fine shrinkage cracks. As the load increased, the participation of the concrete

present in the deck increased. The use of no-shrink concrete in the deck slab may increase the stiffness initially.

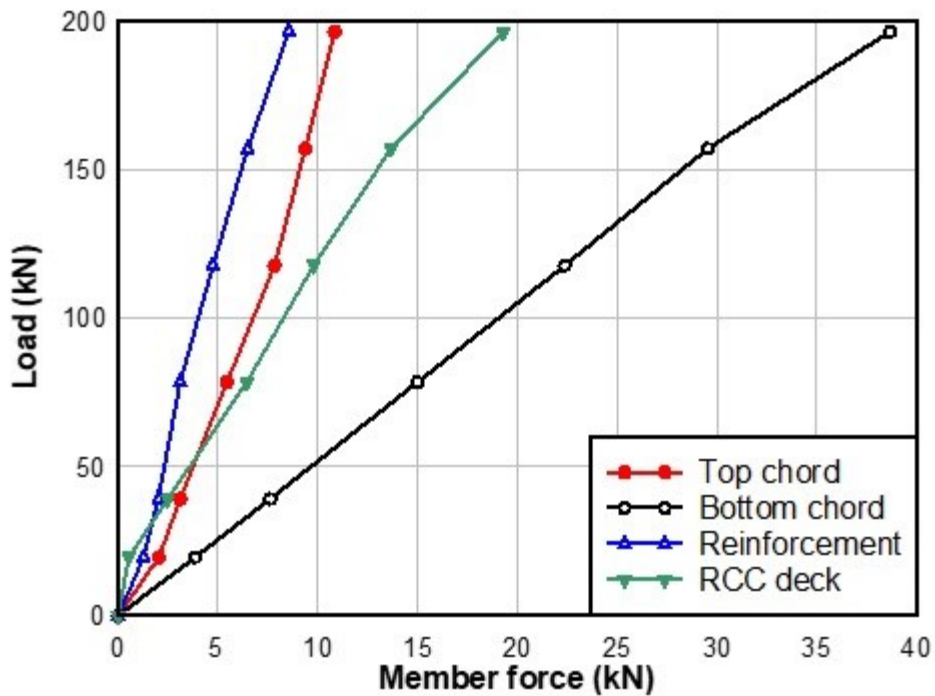


**Figure 4.15:** Load sharing between top chord, bottom chord, reinforcement and concrete deck

#### 4.3.7 Performance of shear studs

Shear studs designed as per IRC 22-2015 satisfactorily performed in the composite truss bridge model up to the failure load with top chord members were well connected with the deck slab and load transfer happened adequately. Therefore, it may be inferred that the spacing of the shear studs suggested by IRC 22-2015 is adequate.

Shear transfer between the steel top chord and RCC deck in the elastic range is an important phenomenon. For a well-designed shear connector arrangement, failure of a composite truss bridge takes place by rupture of the bottom chord, and therefore, plastic redistribution of shear forces in rigid shear studs is not applicable in the case of composite truss bridges.

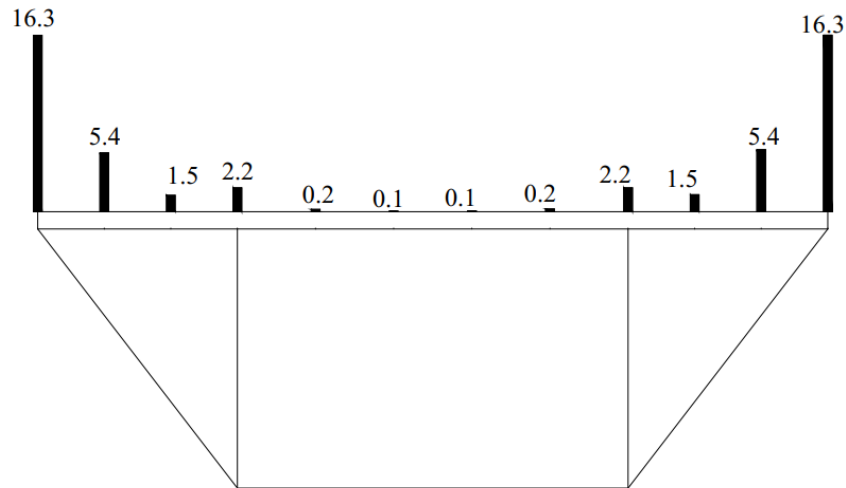


**Figure 4.16** Variation of shear force (kN) in studs as per STAAD

For numerical study on shear stud, the stud was modeled by a beam element. For simplification the number of studs are reduced and the composite slab is assumed to be connected to the top chord only at 12 locations. The size of stud is determined in accordance with the model built for the experiment. The total cross-sectional area of the shear studs connected to one member is equally distributed to 12 locations. This is how solid sections of 9.7mm side, square studs were modeled. Figure 4.16 shows the variation of the shear force in shear studs in the numerical study. It is seen that the force is considerably large near supports and joints as compared to the midsection.

As the STAAD model is validated, the design of shear studs may be carried out based on the shear forces in the studs found from the STAAD analysis. Shear studs may be designed for ultimate load conditions due to the rupture of the central bottom chord member.

